

## COROTATING SHOCKS IN INNER HELIOSPHERE

Y.C. Whang  
Department of Mechanical Engineering  
The Catholic University of America  
Washington, D.C. 20064

### ABSTRACT

This paper reports two possible corotating shocks in the inner heliosphere where the solar wind is composed of low- $\beta$  plasma. In the region where the solar wind is slightly super-Alfvenic, reverse corotating fast MHD shocks can form at the leading edge of a high-speed stream. These shocks possess a switch-on mechanism for amplification of tangential small-scale fluctuations. The second one is the coronal slow shocks which may be imbedded in large coronal holes at low altitude in the sub-Alfvenic region.

### Introduction

In a heliocentric coordinate system corotating with the sun, the large-time-scale structure of the solar wind is often quasi-steady for a few solar rotations. Many large-scale structures of the global solar wind may be treated as steady-state field-aligned flows in a frame of reference corotating with the sun at a constant angular velocity  $\vec{\Omega}$ . The flow velocity in the corotating frame  $\vec{U}$  is either parallel or anti-parallel to the magnetic field  $\vec{B}$ . The solar wind process may be considered to consist of an expansion of the solar wind along each corotating stream tube and a dynamical interaction between neighboring stream tubes.

Recently, magnetohydrodynamic (MHD) treatments have been employed to study the interaction of corotating high-speed streams in the highly super-Alfvenic region of the heliosphere by several authors. For example, Pizzo (1982) has studied some 3D problems under the adiabatic assumption, and Whang and Chien (1981) have studied some MHD interaction problems near the solar equatorial plane to include the heat conduction process.

This paper reports two possible corotating MHD shocks in the low- $\beta$  region of the inner heliosphere. The solar wind flow is sub-Alfvenic near the sun, and a transition from sub-Alfvenic to super-Alfvenic takes place at a heliocentric distance of approximately 0.1 AU. In the slightly super-Alfvenic region, we studied the interaction between two streams of solar wind at different Alfven numbers, a slow stream at a lower Alfven number precedes a fast stream. As a result of interaction, reverse corotating fast MHD shocks may form near 0.1 AU at the leading edge of the high-speed stream. These shocks possess a "switch-on" mechanism for amplification of tangential small-scale fluctuations. The second shock is the coronal slow shock, which may be imbedded in large coronal holes at altitudes of a few solar radii in the sub-Alfvenic region.

## Mathematical Development

The governing equations for the expansion of the solar wind along each stream tube may be represented by a system of five equations. The equation of continuity is

$$\vec{e}_s \cdot \nabla (\rho U/B) = 0 \quad (1)$$

where  $\rho$  is the mass density, and  $\vec{e}_s = \vec{U}/U$  is the unit vector along the streamline direction. The parallel component of the equation of motion is

$$\vec{e}_s \cdot \left( \nabla \frac{U^2}{2} + \frac{1}{\rho} \nabla p - \vec{H} \right) = 0 \quad (2)$$

where  $p$  is the thermal pressure, and

$$\vec{H} = -(GM/r^3) \vec{r} - 2 \vec{\Omega} \times \vec{U} - \vec{\Omega} \times (\vec{\Omega} \times \vec{r})$$

$G$  is the gravitational constant,  $M$  is mass of the sun, and  $\vec{r}$  the heliocentric position vector. The force acting on a unit mass of the solar wind plasma,  $\vec{H}$ , consists of the gravitational force and two fictitious body forces: the coriolis force and the centrifugal force.

The variation of  $p$  and  $\rho$  along each streamline is governed by

$$\vec{e}_s \cdot (\nabla p - c^2 \nabla \rho) = 0 \quad (3)$$

where  $c = (\alpha p/\rho)^{1/2}$  is the sound speed in a heat conducting plasma,  $\alpha$  is the polytropic index. The conduction heat flux is parallel to  $\vec{e}_s$ ,

$$\vec{q} = -\kappa \vec{e}_s \vec{e}_s \cdot \nabla T \quad (4)$$

where  $T$  is the one-fluid temperature, and the thermal conductivity

$$\kappa = K T^{5/2}$$

with  $K = 7.5 \times 10^{-7} \text{ erg s}^{-1} \text{ cm}^{-1} \text{ deg}^{-3.5}$ . The polytropic index is directly related to the variation in thermal state and in heat conduction process along each streamline,

$$\vec{e}_s \cdot \left\{ \left( \frac{5}{3} - \alpha \right) \nabla \rho - \frac{mB}{3kTU} \nabla \left( \frac{q}{B} \right) \right\} = 0 \quad (5)$$

where  $m$  is the proton mass and  $k$  Boltzmann's constant,  $\alpha$  is not a constant along each streamline. In the expansion of the solar wind,  $\alpha < 5/3$  when conduction heat acts as an energy source, it continuously converts into other forms of energy.  $\alpha = 5/3$  in the region where  $\vec{q}$  is a divergence-free vector (including the adiabatic condition with  $q = 0$ ). A special feature of the present formulation of energetics for a heat conducting plasma is the use of a varying polytropic index  $\alpha$  in (3) and (5) instead of the equivalent equation of energy conservation

$$\vec{e}_s \cdot \nabla \left[ \frac{\rho U}{B} \left\{ \frac{U^2 - (\vec{\Omega} \times \vec{r})^2}{2} + \frac{5}{2} \frac{p}{\rho} - \frac{GM}{r} \right\} + \frac{q}{B} \right] = 0$$

From equations (1) - (3), we can obtain

$$\vec{e}_s \cdot \left[ \left( \frac{U^2}{c^2} - 1 \right) \frac{1}{\rho} \nabla p - U^2 \nabla \ln B + \vec{H} \right] = 0 \quad (6)$$

$$\vec{e}_s \cdot \left[ (U^2 - c^2) \nabla \ln \rho - U^2 \nabla \ln B + \vec{H} \right] = 0 \quad (7)$$

and 
$$\vec{e}_s \cdot \left[ (c^2 - U^2) \nabla \ln U - c^2 \nabla \ln B - \vec{H} \right] = 0 \quad (8)$$

$-\vec{e}_s \cdot \nabla \ln B$  measures the rate of fractional change of cross-sectional area of a stream tube along the streamline direction. Once  $\vec{e}_s$  and the variation of cross-sectional area are known, the expansion equations can be integrated along each streamline.

The variation in the direction and the magnitude of the cross-sectional area of each stream tube is controlled by the interaction between neighboring stream tubes (Whang, 1980). The interaction process is governed by the divergence-free condition of the magnetic field.

$$\nabla \cdot \vec{B} = 0 \quad (9)$$

and the dynamical equilibrium of momentum transverse to the streamline direction

$$(U^2 - a^2) \vec{e}_s \cdot \nabla \vec{e}_s + (\vec{I} - \vec{e}_s \vec{e}_s) \cdot \left( \frac{1}{\rho} \nabla p^* - \vec{H} \right) = 0 \quad (10)$$

where  $a = B/(4\pi\rho)^{1/2}$  is the Alfvén speed,  $\vec{I}$  is a unit dyadic, and  $p^* = p + B^2/8\pi$  is the sum of thermal and magnetic pressures. Making use of equation (6), we can write (9) in a new form

$$\left[ U^2 (c^2 + a^2) - c^2 a^2 \right] \nabla \cdot \vec{e}_s + \vec{e}_s \cdot \left[ (U^2 - c^2) \frac{1}{\rho} \nabla p^* + c^2 \vec{H} \right] = 0 \quad (11)$$

The system of the interaction equations, (10) and (11), shows that the variation of the streamline direction is controlled by  $\nabla p^*$  and  $\vec{H}$ . The system is elliptic or hyperbolic, depending on the sign of

$[U^2(a^2 + c^2) - a^2 c^2] / (U^2 - a^2)(U^2 - c^2)$ . It is hyperbolic in the super-Alfvénic, supersonic regime

$$U > \max(a, c)$$

or in a sub-Alfvénic, subsonic regime with

$$\left( \frac{1}{a^2} + \frac{1}{c^2} \right)^{-1/2} < U < \min(a, c)$$

The system of interaction equations is elliptic in other regimes.

In the two hyperbolic flow regimes, solutions of the interaction equations respectively represent families of fast and slow MHD waves. When successive MHD waves travel faster than the preceding ones, they overtake and combine with each other. This phenomenon leads to the formation of fast or slow MHD shocks.

### Corotating Shocks Near 0.1 AU

A simultaneous solution of the expansion equations and the interaction equations is carried out to demonstrate the formation of corotating shock near the equatorial plane in the hyperbolic flow region outside ~0.1 AU where the flow of a low- $\beta$  plasma is supersonic and slightly super-Alfvénic. We assume that near the solar equatorial plane the flow properties are independent of the latitude. Let  $\phi$  denote the directional angle between  $-\vec{r}$  and  $\vec{e}_s$ ,  $\vec{e}_n = \vec{\Omega} \times \vec{e}_s / \Omega$  a unit vector normal to the streamline direction,  $H_s = \vec{e}_s \cdot \vec{H}$  and  $H_n = \vec{e}_n \cdot \vec{H}$ . Then we may write the interaction equations, (10) and (11), near the equatorial plane as

$$(U^2 - a^2) (\vec{e}_s \cdot \nabla \phi - \frac{\sin \phi}{r}) + \frac{1}{\rho} \vec{e}_n \cdot \nabla p^* = H_n \quad (12)$$

and

$$\left[ U^2 (c^2 + a^2) - c^2 a^2 \right] (\vec{e}_n \cdot \nabla \phi + \frac{1 - \cos \phi}{r}) + \frac{1}{\rho} (U^2 - c^2) \vec{e}_s \cdot \nabla p^* = -c^2 H_s \quad (13)$$

In the super-Alfvénic hyperbolic regime, the Mach angle  $\mu$  for fast MHD waves is defined by

$$\cos \mu = (1 - a^2/U^2)^{1/2} (1 - c^2/U^2)^{1/2} \quad (14)$$

We may introduce

$$\vec{c}_{\pm} = \cos \mu \vec{e}_s \pm \sin \mu \vec{e}_n, \quad (15)$$

unit vectors along the two characteristic directions. The characteristic curve defined by  $\vec{c}_+$  running ahead of the streamline in the direction of solar rotation may be called the forward characteristic curve, and that defined by  $\vec{c}_-$  running behind the streamline the reverse characteristic curve. We can express the interaction equations in the form of characteristic equations obtained from a linear combination of (12) and (13),

$$\vec{c}_{\pm} \cdot (\nabla \phi \pm Q \nabla p^*) = S_{\pm} \quad (16)$$

where 
$$Q = \frac{1}{\rho (U^2 - a^2) \tan \mu}$$

and 
$$S_{\pm} = \frac{\cos \mu H_n}{U^2 - a^2} \mp \frac{c^2 H_s}{U^4 \sin \mu} + \frac{1}{r} \left[ \sin(\phi \pm \mu) \mp \sin \mu \right]$$

Solutions for MHD interaction between solar wind streams in the low- $\beta$  region of the inner heliosphere can be obtained from integrations of the expansion equations along streamlines, and integrations of the interaction equations (16) along characteristic curves. A method of solution for solar wind streams in the super-Alfvénic region has been developed previously (Whang and Chien, 1981). The present approach differs from the previous one in two aspects: (i) using a varying polytropic index in (3) and (5) instead of the equivalent equation of energy conservation, and (ii) introducing a new form (11) to represent the divergence-free condition (9). The advantages of the present approach are (i) each of the final interaction equations (16) contains only derivatives along a characteristic direction, and (ii) slow mode MHD waves are not suppressed.

The following numerical solution demonstrates the interaction between two streams of solar wind flow at different Alfvén numbers, in which a slow stream precedes a sharply bounded fast stream of higher Alfvén number. Assume that at the initial surface  $r = 22.5 R_{\odot}$ , the profile for the radial speed (in km/s) be given by

$$U_r = 400 + 8 (1 - \operatorname{erf} \omega)$$

where  $\omega$  is the azimuthal angle in degrees. A smooth increase of the flow speed from  $U_r = 400$  km/s and  $U/a = 1.087$  to  $U_r = 416$  km/s and  $U/a = 1.132$  takes place in a narrow region with its longitudinal width of approximately  $4^\circ$ . We further assume that at the initial surface

$$U_\omega = -\Omega r$$

$$nU_r = 2.795 \times 10^5 \text{ protons cm}^{-2} \text{ s}^{-1}$$

and  $T = 4.3 \times 10^5$  K

From the slow to the fast stream,  $B$  changes from 484 to 439 nT, and  $p^*$  from  $1.016 \times 10^{-6}$  to  $0.847 \times 10^{-6}$  dyne/cm<sup>2</sup>.

We have obtained the numerical solution for all flow parameters in the region  $22.5 \leq r/R_{\odot} < 30.4$ . In the top frame of Figure 1 are plotted the streamlines (in heavy curves) and the two families of characteristic curves in the physical plane. The streamline passing through  $\omega = 0$  at the initial surface is identified as the central streamline. At the initial surface, the Mach angle decreases across the interface from  $\mu = 83.6^\circ$  in the slow stream to  $\mu = 62.8^\circ$  in the fast stream due to changes in Alfvén numbers. Thus the slopes of those characteristic curves starting near the initial interface change rapidly. The merging of the reverse characteristic curves shown in the plot indicates the formation of a reverse corotating shock, it signifies a piling up of the fast-mode MHD waves to form a fast MHD shock. The lower frame of Figure 1 shows the profile of the total pressure  $p^*$  at various heliocentric distances. Shock fronts with steep profiles of  $p^*$  appear at the leading edge region. The shock fronts become broader and weaker at approximately  $15^\circ$  (or ~24 hours) behind the central streamline due to geometrical effects. Unlike the total pressure, other flow properties ( $U$ ,  $\rho$ ,  $T$ , etc.) change abruptly across the stream interface around the central streamline. Disturbances of flow proper-

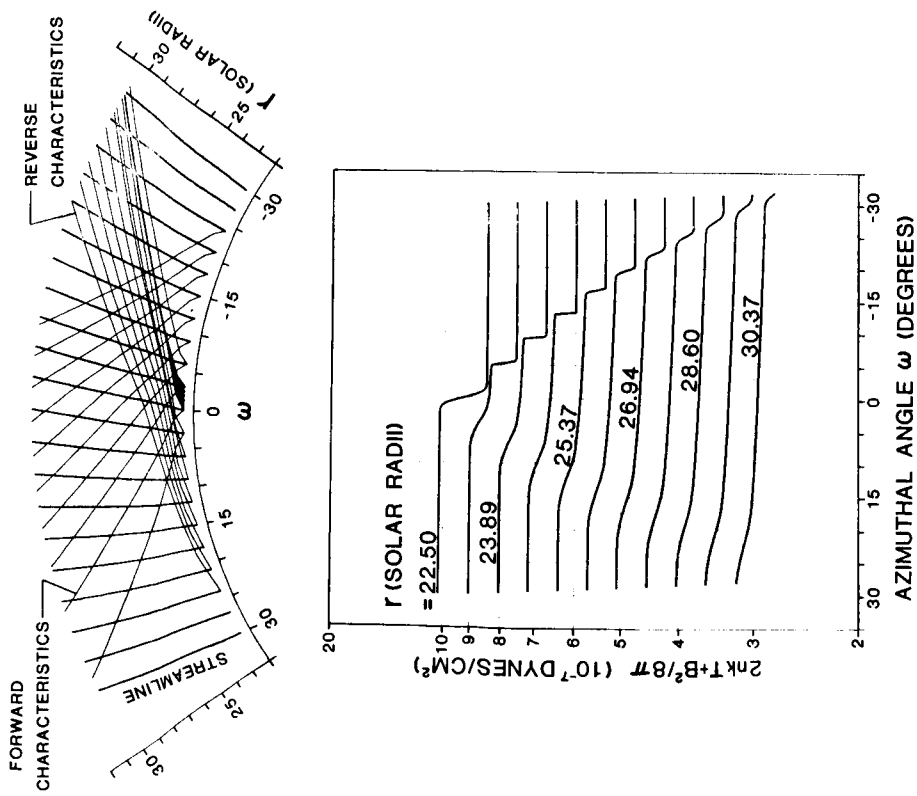


Figure 1. The top frame shows the streamlines and characteristic curves. The merging of the reverse characteristic curves signifies the formation of a reverse corotating shock at the leading edge. The lower frame shows the profile of  $p^*$  at the shock front.

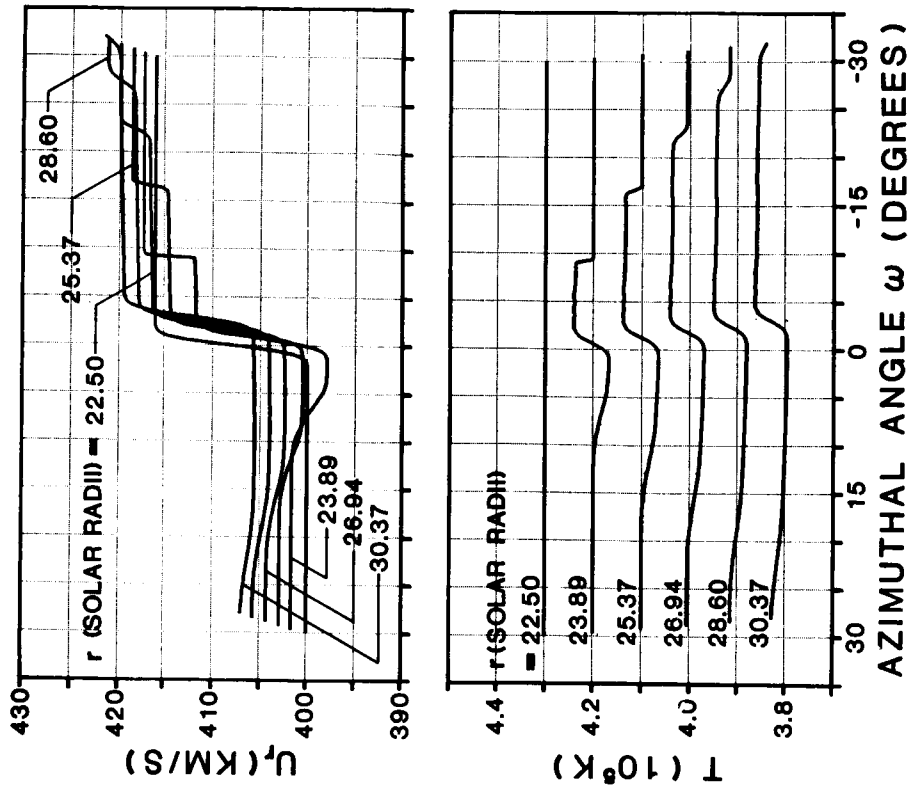


Figure 2. The radial velocity and the temperature in the interaction region. The shocked plasma between the central streamline and the reverse corotating shock has a higher temperature than its surroundings.

erties due to stream interaction are confined to an interaction region bounded by the two characteristics which intersect the initial surface near the central streamline. The solar wind streams undergo a simple expansion process without strong interaction between neighboring stream tubes outside of the interaction region. In the region where the flow is slightly super-Alfvenic, one can distinguish clearly the shock front from the interface because of large Mach angles. Between the interface and the reverse shock, the flow properties carry the signatures of a shocked plasma as shown in Figure 2, which plots the profiles of  $U_r$  and  $T$  at various heliocentric distances. Although the temperature is assumed to be uniform at the initial surface, the shocked plasma has a higher temperature in the leading edge region.

This example illustrates that in the low- $\beta$  region of the inner heliosphere where the solar wind flow is slightly super-Alfvenic, if the Alfven number increases at the leading edge region of a high-speed stream even at a very slow rate, reverse corotating shocks may form in the region. These shocks are fast MHD shocks of low- $\beta$  plasma, with the upstream normal Mach number slightly greater than 1. They are capable of amplifying the tangential component of the magnetic field. Thus, the presence of a small random fluctuation field upstream of these shock surfaces can be amplified to produce a large, tangential fluctuation field downstream of the shock. This effect may be called a switch-on mechanism, which will be discussed in detail in a separate paper. This amplification mechanism is probably responsible for the presence of large-amplitude anisotropic fluctuations observed at the leading edge of high-speed streams (Belcher and Davis, 1971).

#### Coronal Slow Shocks

At altitudes of a few solar radii, the solar wind is a sub-Alfvenic low- $\beta$  plasma. It has been suggested that, in this region of the inner heliosphere, corotating slow MHD shocks might be imbedded within large polar coronal holes (Whang, 1982).

Figure 3 depicts the geometry of a coronal slow shock around a simple two-hole corona. The solar wind originating from open-field coronal holes is accelerated to high speeds at low altitudes in the corona. Streams originating from the edge of the polar open-field regions flow around the curved boundary of the helmet-shaped, closed-field region (Pneuman and Kopp, 1971). Near the inner edge of the neutral sheet, the flow direction of each stream changes suddenly, becoming parallel to the neutral sheet. An oblique slow shock can develop near or at the neutral point. The shock extends polewards to form a composite surface of discontinuity surrounding the sun. These standing shocks could occur quite close to the solar surface, at 2 to 5 solar radii above large coronal holes. Numerical solutions have been constructed for the expansion of the solar wind in open field region of the solar corona along stream tubes with prescribed geometry by Pneuman and Kopp (1971) and by Whang (1983). These solutions did not consider dynamical interaction between neighboring stream tubes, and their streamline geometry was introduced under an *a priori* assumption that no shocks exist in the corona.

For not very large coronal holes, the coronal slow shocks are weaker at lower altitudes, and could have a partially concave surface as shown in Figure 4.

### CORONAL SLOW SHOCKS

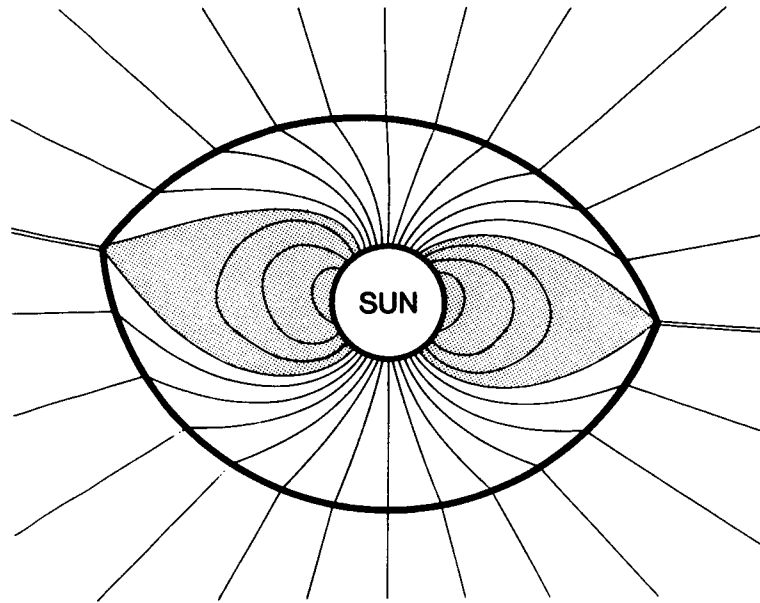


Figure 3. The geometry of a slow shock in a corona with two large polar holes.

### CORONAL SLOW SHOCK

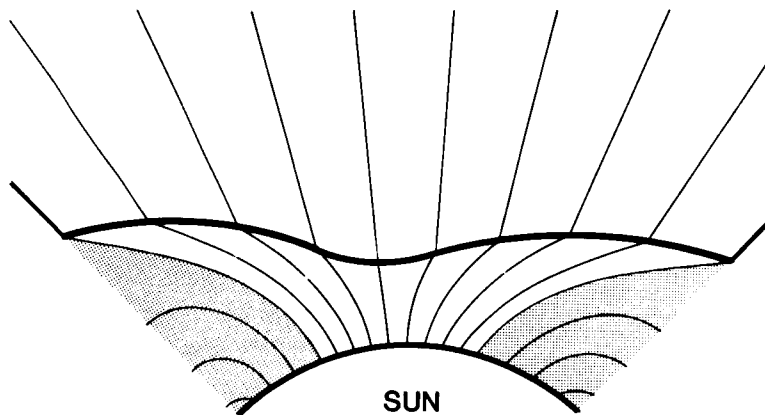


Figure 4. For not very large coronal holes, the slow shocks are weaker at lower altitudes, and could have a partially concave shock surface.

Let  $\theta$  denote the angle between the magnetic field and the shock normal, and  $C_s$  be the normal slow speed,

$$C_s^2 = \frac{1}{2} (a^2 + c^2) - \frac{1}{2} \left\{ (a^2 + c^2)^2 - 4a^2 c^2 \cos^2 \theta \right\}^{\frac{1}{2}}$$

The normal component of the flow speed  $U_n$  is greater than  $C_s$  upstream, and less than  $C_s$  downstream of a slow MHD shock. The flow downstream of a slow shock is hyperbolic, sub-Alfvénic and subsonic. In the hyperbolic flow region, solutions of the interaction equations (10) and (11) represent (obtuse) Mach angle  $\mu$  with

$$\cos \mu = - \left( \frac{a^2}{U^2} - 1 \right)^{\frac{1}{2}} \left( \frac{c^2}{U^2} - 1 \right)^{\frac{1}{2}} \quad (17)$$

(Sears and Resler, 1961). Successive slow waves travel upstream faster than the preceding ones, so that they overtake and combine with each other to form a slow shock upstream of the sub-Alfvénic and subsonic hyperbolic flow region.

In contrast with the jump conditions for fast MHD shocks,  $B$  and  $\theta$  decrease across a slow shock.  $\beta$  increases due to the sudden rise in the thermal pressure and the drop in the magnetic pressure. However,  $p^*$ , as well as  $\rho$  and  $T$ , always increase. The possible existence of coronal slow shocks can significantly revise our understanding on the dynamical structure of the global solar wind.

Acknowledgements. The author is indebted to Drs. L.F. Burlaga and N.F. Ness for their help and suggestions. The numerical solutions were carried out using the computer facility at NASA-Goddard Space Flight Center. This research was supported in part by the National Aeronautics and Space Administration under Grant NSG-7422 and, in part, by the Atmospheric Sciences Section of the National Science Foundation under NSF Grant ATM-8119302.

#### References

- Belcher, J.W., and L. Davis, Jr., Large-Amplitude Alfvén Waves in the Interplanetary Medium, 2, J. Geophys. Res., 76, 3534, 1971.
- Pizzo, V.J., A Three-Dimensional Model of Corotating Streams in the Solar Wind, 3, Magnetohydrodynamic Streams, J. Geophys. Res., 87, 4374, 1982.
- Pneuman, G.W., and R.A. Kopp, Gas-Magnetic Field Interaction in the Solar Corona, Solar Phys., 18, 258, 1971.
- Sears, W.R., and E.L. Resler, Jr., Sub- and Super-Alfvénic Flows Past Bodies, Adv. Aerospace Sci., 3-4, 637, 1961.
- Whang, Y.C., A Magnetohydrodynamic Model for Corotating Interplanetary Structures, J. Geophys. Res., 85, 2285, 1980.
- Whang, Y.C., and T.H. Chien, Magnetohydrodynamic Interaction of High-Speed Streams, J. Geophys. Res., 86, 3263, 1981.
- Whang, Y.C., Slow Shocks Around the Sun, Geophys. Res. Letters, 9, 1081, 1982.
- Whang, Y.C., Expansion of the Solar Wind from a Two-Hole Corona, to appear in Solar Phys., 1983.